



REGULAR ARTICLE

Low-Profile Tapered Slot Antenna for Wearable Military Applications

M. Benisha¹, C. Priya², T. Annalakshmi³, Kumutha Duraisamy^{1,*} ,
Delshi Howsalya Devi. R⁴, Manjunathan Alagarsamy⁵

¹ Department of ECE, Jeppiaar Institute of Technology, Kunnam, Sriperumbudur, TN, India

² Department of ECE, Karpagam College of Engineering, Coimbatore, TN, India

³ Department of ECE, S.A Engineering College, Thiruverkadu, Chennai, TN, India

⁴ Department of AI&DS, Karpaga Vinayaga College of Engineering and Technology, Chengalpattu, TN, India

⁵ Department of ECE, K. Ramakrishnan College of Technology, Trichy, TN India

(Received 07 April 2025; revised manuscript received 15 June 2025; published online 27 June 2025)

This paper presents a low-profile tapered slot antenna (TSA) designed for wearable military applications, offering a compact, lightweight, and flexible solution for tactical communication systems. The antenna operates over a wide frequency range, ensuring compatibility with various military communication bands. It is designed using a flexible substrate, enabling seamless integration with wearable gear while maintaining stable performance under bending conditions. Advanced miniaturization techniques are employed to achieve a low-profile structure without compromising gain or efficiency. Experimental results confirm stable impedance matching, high gain, and low cross-polarization levels. The designed single element of Vivaldi antennas has been fabricated. The return loss response and radiation patterns of the constructed antennas and the Single Element Antenna are measured and compared to simulated findings. The fabricated antenna provides a return loss of -23 dB and a gain of 8 dB, which is suitable for wearable military applications. The robust design withstands harsh environmental conditions, making it ideal for field operations. This work provides a promising solution for next-generation wearable communication systems

Keywords: Wireless Communication (WC), Wearable communication, Vivaldi antenna, VSWR, Military applications.

DOI: [10.21272/jnep.17\(3\).03017](https://doi.org/10.21272/jnep.17(3).03017)

PACS numbers: 73.61.Jc, 71.20.Mq,
88.40.jj, 88.40.hj

1. INTRODUCTION

Military applications demand robust, reliable, and secure communication systems. Wearable antennas in military contexts must operate effectively in diverse environments, resist harsh conditions, and ensure minimal detection by adversaries [1, 2].

Integrating low-profile Vivaldi antennas into wearable military gear involves addressing challenges such as maintaining antenna performance despite body loading, ensuring flexibility and durability, and minimizing the antenna's detectability [3, 4]. Recent advancements focus on materials science for better flexibility, metamaterials for enhanced performance, and integration with other wearable technologies such as sensors and power systems [5, 6]. Key challenges include ensuring antenna performance under various body conditions, minimizing power consumption, enhancing durability against environmental factors, and integrating seamlessly with existing military gear [7, 8]. Gazit [9] proposed two important changes to the traditional Vivaldi design. He used a low dielectric substrate (cuclad, $\epsilon = 2.45$) instead of alumina and an antipodal slotline transition. The antipodal slotline transition was constructed by tapering the microstrip line through parallel

strip to an asymmetric double sided slot line. This type of transition offered relatively wider bandwidth which was restricted by the microstrip to slotline transition of the traditional design. However, antipodal slotline transition had the problem of high cross polarization.

Langley et al. [10] improved the antipodal transition of E. Gazit with a new and balanced structure to improve the cross-polarization characteristics. This type of structure, known as balanced antipodal transition, consists of three layers of tapered slots fed directly by a stripline. E-field distribution of the antipodal transition is balanced with the addition of the mentioned layer. The tapered slots on both sides of the antenna serve as ground planes. The balanced antipodal transition offered a 18:1 bandwidth with fairly well cross polarization characteristics. Then, Langley et al. [10] also constructed a wide bandwidth phased Single Element Antenna using this balanced antipodal Vivaldi antenna. He achieved good cross polarization levels as well as wideband wide-angle scanning.

2. PRINCIPAL OF OPERATION OF VIVALDI ANTENNA

The Vivaldi antenna belongs to the surface wave class of traveling wave antennas (the other traveling

* Correspondence e-mail: skvijaykumu@gmail.com



wave antenna type is the leaky wave antenna). In order to describe principle of operation, the surface wave antennas can be divided into two sections: propagating section and radiating section. The slot width (separation between the conductors) is smaller than one-half free space wavelength ($\lambda_0/2$) and the waves traveling down the curved path along the antenna are tightly bound to the conductors in the propagating section. The bond becomes progressively weaker, and the energy gets radiated away from the antenna coupling to the air in the radiating section where the slot width is increasing beyond the one-half wavelength. The waves are traveling along the antenna surface until the limiting case of phase velocity is equal to the free space velocity of light ($c = 3 \times 10^8$). The limiting case intends the antenna with air as dielectric. Radiation from low dielectric substrates is considerably high and crucial for the antenna operation.

Feeding approaches can be classified into two types: directly coupled transitions and electromagnetically coupled transitions. In directly coupled transitions a wire or a solder connection can act as the direct current path providing the electrical contact for this type of transition. The best known directly coupled transition type is coaxial line to slotline transition. In Coaxial to Slotline Transition of transition, the signals are coupled to the slotline from the actual antenna feed through a coaxial line. An open circuited slot and a coaxial line placed perpendicular to it form the transition. The electrical connection of the coaxial cable to the ground plane is provided by the outer conductor on one side of the slot while the inner conductor of the cable is placed over the slot forming a semicircular shape [11]. The characteristic impedance of the slotline is too high to get an adequate matching characteristic with the slotline etched on single side of the substrate. A better matching, thereby a wider bandwidth, is obtained etching the slotline on both sides of the substrate. However, coaxial feeding is still unfavorable to implement successfully due to etching difficulties [12-15]. The coupling of signals in Electromagnetically Coupled Transitions. Microstrip to slotline, stripline to slotline, antipodal slotline and balanced antipodal slotline are the best known types of electromagnetically coupled transitions.

The basic microstrip to slotline transition is constructed with microstrip and slotline crossing each other at a right angle. The microstrip is etched on one side of the substrate and the slotline on the other side of the substrate. The microstrip crosses the slotline and extends one quarter of a wavelength further from the slotline in the same way as the slotline extending one quarter wavelength further from the microstrip. The quarter wavelength microstrip stub is open circuited but appears as a short circuit at the crossing with slotline[16-18]. The slotline stub is bonded to the ground plane and short circuited but obviously it appears as an open circuit at the crossing. This mechanism makes electromagnetic coupling between the microstrip and the slotline possible. Figure 1 shows the basic microstrip to slotline transition structure.

This kind of transition reduces the operating bandwidth considerably. Six-port microstrip to slotline transition was proposed by Scieck and Kohler [12] to overcome this problem. However, the transitions of these six

ports are too difficult to implement. The structure is shown in Figure 2. below.

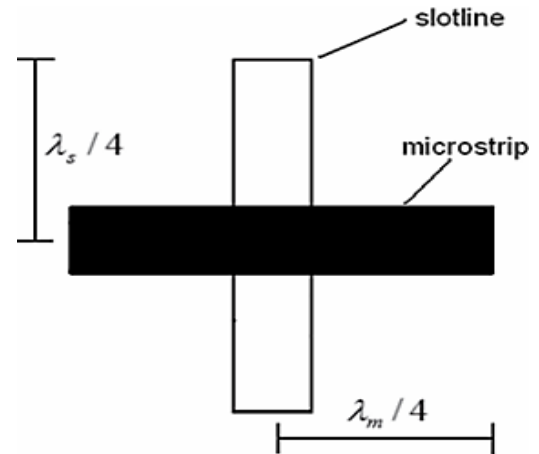


Fig. 1 – Microstrip to slotline transition

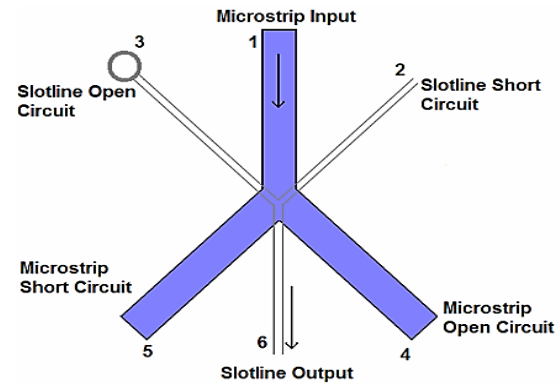


Fig. 2 – Six-port microstrip to slotline transition

3. PROPOSED DESIGN

3.1 Stripline Model

First of all, a model is formed to match the characteristic impedance of the stripline to that of the transmission line (feeding the antenna) and the slotline. The substrate material (dielectric constant) and thickness as well as the stripline width determine the characteristic impedance of the structure. Thus, the model consists of the antenna substrate and the stripline only since the whole antenna model will be inessential to find the characteristic impedance of the feeding section. Determining these parameters, the stripline model shown in Figure 3 is employed.

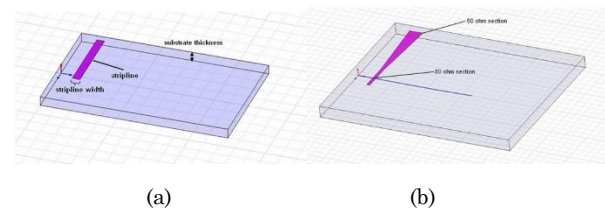


Fig. 3 – (a) Stripline model, (b) Stripline model with 80 Ω to 50 Ω transition

Stripline will be designed to have 50 Ω characteristic impedance both in the slotline transition and the input

of feeding section as stated earlier in this chapter. characteristic impedance in the feeding as seen in Figure 3. This method provides a considerable bandwidth increase. However, 50 Ω characteristic impedance through the complete stripline will provide the bandwidth requirement.

Among the substrates with dielectric constant in the range of 2.2 to 10.2, Rogers RT/duroid™ 5880 has the minimum tangent loss ($\tan \delta = 0.0009$) and a dielectric constant of $\epsilon_r = 2.2$. Rogers RT/duroid™ 5880 is chosen as the substrate material to be used in this work. In this design, two 0.062" (1.570mm) ±0.002" thick boards are to be used, i.e. the substrate thickness is 0.124" (3.140 mm). An improvement in the performance is obtained using thicker substrates due to a decrease in the antenna reactance through the whole band. Table 1 gives the calculated and simulated characteristic impedance of the stripline for various stripline width where 3.14 mm thick Rogers RT/duroid™ 5880 dielectric is used. Simulations are carried out using Ansoft ADS®.

Table 1 – Change in characteristic impedance of the stripline with stripline width

W_{ST} (mm)	1.5	2.0	2.5	3.0
Z_0 (Ω) (simulated)	65.605	57.283	50.27	44.107
Z_0 (Ω) (calculated)	69.28	59.06	51.47	45.60

3.2 Stripline and Slotline Model

In this part, the feeding section of the antenna is modelled. The model is formed cascading two identical transitions designed. Thus, both return loss ($20\log S_{11}$) and reverse gain (insertion loss or $20\log S_{21}$) of the antenna might be analysed of the mentioned system. The return loss and reverse gain responses of this model are expected to be close to the complete antenna performance since the stripline model parameters and the parameters to be specified here mainly determines the return loss response and the reverse gain of the design. Figure 4 shows the cascaded transitions model.

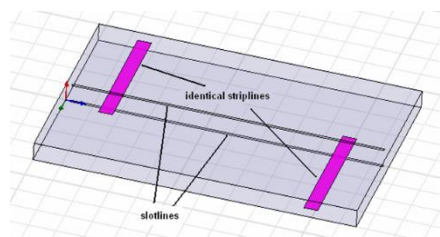


Fig. 4 – Cascaded identical transitions

3.3 Fabricated Antenna

The single element Vivaldi antennas and the improved Single Element Antenna detailed above are fabricated in Aselsan Inc. using printed circuit board technology. The fabricated Antenna is shown below Fig. 5.

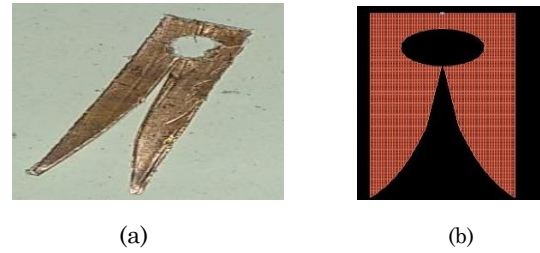


Fig. 5 – (a) Fabricated of single element antenna design. (b) Simulated of single element antenna design

4. FABRICATED RESULTS

The return loss response of the final Vivaldi antenna design demonstrates its effective impedance matching across the operational frequency range. The response exhibits a return loss below -10 dB across the targeted frequency bands, indicating minimal reflection and efficient power transfer as shown in Figure 6. Peaks in the return loss curve highlight the antenna's strong resonance at specific frequencies. This performance ensures reliable communication for wearable military applications. The design also maintains stable impedance characteristics under bending conditions, making it suitable for wearable use cases.

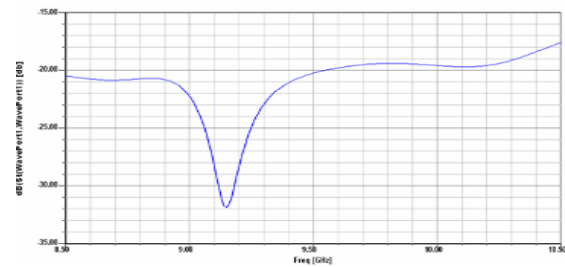


Fig. 6 – Return loss response of the final design

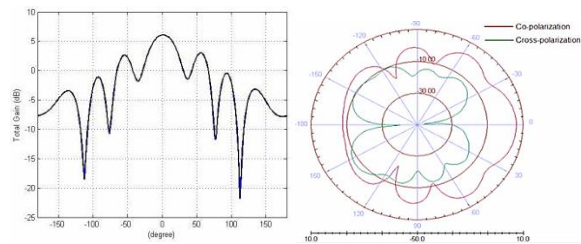


Fig. 7 – H -plane total radiation pattern and co-polarization and cross-polarization patterns of final design at 8.5 GHz

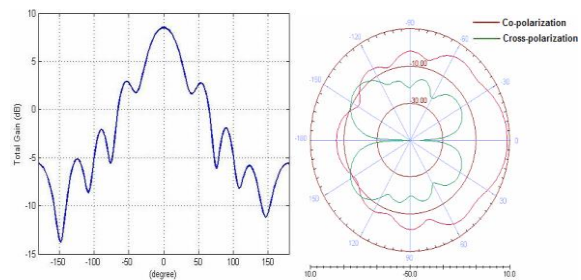


Fig. 8 – H -plane total radiation pattern and co-polarization and cross-polarization patterns of the final design at 9.5 GHz

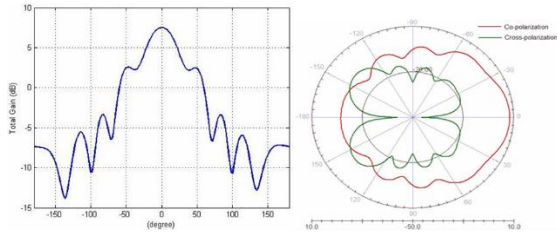


Fig. 9 – H -plane total radiation pattern and co-polarization and cross-polarization patterns of final design at 10.5 GHz

The H -plane radiation pattern of the final Vivaldi antenna design at 8.5 GHz, 9.5 GHz and 10.5 GHz respectively are shown in Figures 6 to 8, which exhibits a stable directional radiation characteristic, suitable for wearable tactical applications. The co-polarization pattern demonstrates strong radiated power in the desired direction, ensuring efficient signal transmission. In contrast, the cross-polarization levels remain significantly lower, indicating minimal polarization losses and high purity of the transmitted signal. This balance between co-polarization and cross-polarization confirms the antenna's capability

REFERENCES

1. Y. Lin, Q. Zhou, C. Xu, *IEEE Commun. Magaz.* **53** No 3, 20 (2015).
2. Y. Wang, X. Luo, *IEEE Access* **6**, 34375 (2018).
3. T. Nguyen, H. Lee, *IEEE Trans. Milit. Commun.* **2** No 1, 45 (2021).
4. P. Sharma, A. Kumar, *Int. J. Anten. Propag.* **2022**, 1234567 (2022).
5. L. Zhao, Y. Zhang, *IEEE Trans. Anten. Propag.* **71** No 3, 1524 (2023).
6. R. Patel, M. Singh, *IEEE Access* **11**, 67890 (2023).
7. M. Garcia, F. Torres, *IEEE Anten. Propag. Magaz.* **65** No 2, 50 (2023).
8. D. Kumutha, R. Delshi Howsalya Devi, et al., *J. Nano-Electron. Phys.* **16** No 4, 04003 (2024).
9. M. Jeyabharathi, D. Kumutha, et al., *J. Nano-Electron. Phys.* **16** No 3, 03008 (2024).
10. B.I.I. Aljidi, S. Perumal, S.A. Pitchay, *Indonesian Journal of Electrical Engineering and Computer Science (IJECS)* **28** No 3, 1573 (2022).
11. S. Perumal, *International Journal of Interactive Mobile Technologies* **16** No 9 (2022).
12. D. Kumutha, T. Islam, et al., *J. Nano-Electron. Phys.* **16** No 3, 03010 (2024).
13. Q. Huang, S. Li, *IEEE Trans. Defense Secur.* **3** No 1, 10 (2024).
14. D. Kumutha, N. Amutha Prabha, *J. Ambient. Intell. Human. Comput.* (2017).
15. I. Shammugam, G.N. Samy, P. Magalingam, N. Maarop, S. Perumal, B. Shanmugam, *Indonesian Journal of Electrical Engineering and Computer Science* **21** No 3, 1820 (2021).
16. J.D.S. Langley, P.S. Hall, P. Newham, *Electron. Lett.* **29** No 23, 2004 (1993).
17. S. Al Perumal, M. Tabassum, N.M. Norwawi, G.A.N. Samy, *2018 8th IEEE International Conference on Control System, Computing and Engineering (ICCSCE)*, 70 (2018).
18. B. Schiek, J. Kohler, *IEEE Trans. Microwave Theory Tech.* **24** No 4, 231 (1976).

Низькопрофільна кінчна щілинна портативна антена для військових застосувань

M. Benisha¹, C. Priya², T. Annalakshmi³, Kumutha Duraisamy¹,
Delshi Howsalya Devi. R⁴, Manjunathan Alagarsamy⁵

¹ Department of ECE, Jeppiaar Institute of Technology, Kunnam, Sriperumbudur, TN, India

² Department of ECE, Karpagam College of Engineering, Coimbatore, TN, India

³ Department of ECE, S.A Engineering College, Thiruwerkadu, Chennai, TN, India

⁴ Department of AI&DS, Karpaga Vinayaga College of Engineering and Technology, Chengalpattu, TN, India

⁵ Department of ECE, K. Ramakrishnan College of Technology, Trichy, TN India

У цій статті представлена низькопрофільна кінчна щілинна антена (TSA), розроблена для портативного використання, яка пропонує компактне, легке та гнучке рішення для тактичних систем зв'язку. Антена працює в широкому діапазоні частот, забезпечуючи сумісність з різними діапазонами зв'язку. Вона розроблена з використанням гнучкої підкладки, що дозволяє безшовну інтеграцію з носимим обладнанням, зберігаючи стабільну роботу в умовах вигину. Для досягнення низькопрофільної структури без шкоди для коефіцієнта посилення або ефективності використовуються передові методи мініатюризації. Експериментальні результати підтверджують стабільне узгодження імпедансу, високий коефіцієнт посилення та низький рівень крос-поляризації. Виміряні характеристики втрат на відбиття та діаграми спрямованості побудованих антен та одноелементної антени, які порівнюються з результатами моделювання. Виготовлена антена забезпечує втрати на відбиття -23 дБ та коефіцієнт посилення 8 дБ.

Ключові слова: Бездротовий зв'язок, Переносні пристрої, Антена типу Вівальді, КСХН, Тактична антена.